Available online at www.sciencedirect.com
SCIENCE DIRECT
Surface Science 600 (2006) 1579–1585
SURFACE SCIENCE
www.elsevier.com/locate/susc

Lifted reconstruction as a feedback mechanism in the oscillating CO oxidation on Pt nanofacets: Microscopic evidences

Y. Suchorski [a,*], W. Drachsel [a,1], V.V. Gorodetskii [b], V.K. Medvedev [c], H. Weiss [a]

[a] Chemisches Institut, Otto-von-Guericke-Universität Magdeburg, Universitätsplatz 2, D-39106 Magdeburg, Germany
[b] Boreskov Institute of Catalysis, Russian Academy of Sciences, Prosp.Lavrentieva 5, RU-630090 Novosibirsk, Russia
[c] Department of Chemical Engineering, University of Washington, Box 351750, Seattle, WA 98195-1750, USA

Available online 24 February 2006

Abstract

Global and local oscillations in the CO oxidation reaction have been visualized in situ on the apex of a [1 0 0]-oriented Pt field emitter tip used as a well-defined model for catalytically active, nm-sized particles by Field Emission (FEM) and Lithium Field Desorption (Li-FDM) Microscopes. For the first time experimental evidence is provided that the reconstruction feedback mechanism of the self-maintained oscillations for the [1 0 0] and [1 1 0] orientations, which is well established on macroscopic single crystals, is also valid in the heterogeneous, nm-sized system with its different crystallographic orientations which are coupled by surface diffusion.

Keywords: Field emission microscopy; Field desorption microscopy; Surface chemical reaction; Surface relaxation and reconstruction; Catalysis; Platinum; Alkali metals

1. Introduction

The idea of adsorption-induced modifications of the total surface energy, and thus of adsorption-modified interatomic interactions within the topmost surface layer, suggested by Irving Langmuir in his Nobel Lecture in 1932, has been impressively confirmed decades later in a direct LEED examination of the adsorption-induced Ni(1 1 0) reconstruction by Germer and MacRae [1]. Again decades later the adsorption-lifted reconstruction of Pt(1 0 0) and Pt(1 1 0) surfaces was found to play a decisive role in self-sustaining oscillations in the CO oxidation reaction on macroscopic Pt(1 0 0) and Pt(1 1 0) single crystal surfaces [2,3]. Such spontaneously oscillating surface reactions on well-defined surfaces provide manifold examples of spiral and standing waves, target patterns and other spatiotemporal structures, and are almost perfect paradigms for understanding the complex reaction–diffusion systems [4,5]. The above experimental observations could be also nicely described within the mean-field theoretical models [6,7].

Two key phenomena lead to rate oscillations in the CO oxidation on macroscopic Pt(1 0 0) and Pt(1 1 0) surfaces which proceeds via the Langmuir–Hinshelwood mechanism: asymmetric inhibition and lifted reconstruction. Asymmetric inhibition of the dissociative oxygen adsorption by CO provides the bistability in the reaction system. Since O_2 needs two adsorption sites per molecule and can hardly adsorb on a densely CO-covered surface, two stable states of the reaction system, with high and low reactivity, coexist over a range of operating conditions. To exhibit oscillations, the system requires apart of a bistability a negative feedback mechanism [8]. In case of the Pt(1 0 0) surface this is provided by a lifting of the "hex" reconstruction of the Pt(1 0 0) surface which is induced by adsorbed CO_{ad}, i.e. a hex $\rightarrow 1 \times 1$ structural phase transition, which

* Corresponding author. Tel.: +49 391 6718824; fax: +49 391 6711396.
E-mail address: yuri.suchorski@vst.uni-magdeburg.de (Y. Suchorski).
[1] On leave from: Fritz-Haber-Institut der Max-Planck-Gesellschaft, Berlin, Germany.

0039-6028/$ - see front matter © 2006 Elsevier B.V. All rights reserved.
doi:10.1016/j.susc.2005.11.060

is accompanied by a drastic increase in the sticking coefficient for oxygen from $\approx 10^{-4}$–10^{-3} for the "hex" to ≈ 0.3 in case of the 1×1 structure [9,10], respectively, and thus in the surface reactivity. In case of Pt(1 1 0) it is the CO_{ad}-induced "missing row" $1\times2 \rightarrow 1\times1$ transition, where the structure-sensitive sticking coefficient for oxygen increases from ≈ 0.3–0.4 to ≈ 0.6 [11]. A very fast catalytic surface process (clean-off reaction) removes then the CO_{ad} layer, and the clean unstable 1×1 surface reconstructs again closing the oscillating cycle. The periodic switching between states of low and high reactivity provides a feedback loop in the system, and induces the oscillations. The validity of the depicted mechanism for "macroscopic" single crystals was directly confirmed by in situ LEED measurements that have attributed the structural changes of the substrate to the reaction rate oscillations [12,13].

Despite of the tacit assumption that an oscillating reaction kinetics, including the described feedback mechanism, should also be valid in the CO oxidation on the nm-sized facets of "real catalyst" Pt particles, no experimental evidence has been provided so far (a kind of a "materials gap" problem). However, since the most characteristic property of such a metal particle is the presence of differently oriented facets which are confined by stepped regions, the oscillations on a nanosized heterogeneous sample might also be induced by reaction–diffusion processes coupled in a complex manner. Moreover, because of the increasing role of fluctuations, significant deviations from the "macroscopic" reaction behaviour are expected [14]. Therefore, alternative mechanisms related to the coupling of the different crystallographic orientations need to be taken into consideration, too [15].

In the present study a Pt field emitter tip was chosen as model system in order to study the possible feedback mechanisms in a nm-sized system. The apex of a field emitter tip exhibits a heterogeneous surface formed by differently oriented nanofacets, and can thus serve as a suitable model for a catalytic particle of comparable dimensions. However, in contrast to a catalyst particle, the tip surface can be prepared reproducibly and can be characterized with atomic resolution by Field Ion Microscopy (FIM). We use Field Emission (FEM) and Lithium Field Desorption (Li-FDM) Microscopy to visualize in situ the oscillating CO oxidation on the Pt nanofacets and to obtain direct real-time information about the actual configuration of the surface during the ongoing reaction. The reconstruction (including adsorption-induced transitions) of the various Pt-metal surfaces have been identified earlier in FIM [16,17], but not yet under the reaction conditions, where the elevated temperature impedes the atomic resolution.

2. Experimental

Experiments were performed in a stainless steel FIM apparatus (base pressure $\leqslant 10^{-10}$ mbar) that was used as a flow reactor. The Pt catalyst sample was the apex of a [1 0 0]-oriented tip etched from a spectroscopically pure Pt wire (0.1 mm ∅) and characterized with atomic resolution in Ne^+ FIM at 78 K. For imaging of the surface with Li^+ ions in Li-FDM, a submonolayer Li (0.1–0.4 ML) was deposited onto the tip from a commercial Li source (SAES Getters). The resulting Li coverage was estimated from the work function measured in the FEM mode, which could be switched on by simply reversing the tip voltage polarity.

In the Li-FDM mode, lithium adatoms are field-desorbed from the apex of the tip as Li^+ ions which in turn create a (channel–plate intensified) projection of the adsorption sites on the fluorescent screen (see Fig. 1). Removed Li adatoms are replaced by diffusion of Li over the tip surface from the long-lasting Li deposit on its shank. Since the tip assembly and the controlling electronics allow temperatures between 78 and 600 K (maintained with an accuracy $\leqslant 1$ K), the surface diffusion rate of Li from the supply on the shank to the imaged surface sites can be precisely adjusted. The Li^+ desorption rate depends nearly exponentially on the desorbing field strength and can thus be controlled by the externally applied field (usually 5–10 V/nm) and by the tip temperature. Local field deviations caused by the peculiarities of the surface structure influence the local Li^+ ion emission, an effect which we use here for the detection of the surface reconstruction.

The UHV system was equipped with a gas supply system for an imaging gas (Ne, for the FIM imaging of the tip structure) and the gases used in the reaction (CO, O_2) which were introduced with a flow rate of 2.5 ls^{-1} and controlled by a spinning rotor gauge and a quadrupole mass spectrometer. The specifics of the visualization of the CO oxidation reaction by FEM, FIM and Li-FDM are described explicitly in the Refs. [18,19].

The Li-FDM, FIM and FEM images were recorded during the ongoing reaction by means of a CCD camera with 40 ms time resolution and digitized with 8 bit resolution. Rectangular probe regions (ROIs – "Regions Of Interest") could be deliberately chosen whose location and size were determined by overlapping the Li-FDM image with a low-temperature FIM image of the same tip. Typically, the size of the probed area was equal to or less than about 500 nm^2. More details of the digitization procedure can be found elsewhere [20].

3. Results and discussion

The Langmuir–Hinshelwood mechanism of the oscillating CO oxidation reaction on Pt requires adsorption of both reactants, CO and oxygen, on the surface. In a simplified description, an O_{ad} and a CO_{ad} layer replace each other periodically during the oscillations by a mechanism described above, and due to the diffusional coupling most of the facets present on the tip are involved in the process. Since the work function of the oxygen-covered Pt surface is remarkably higher than that of a CO-covered surface, the oscillation can be monitored by FEM due to the high sensitivity of the field electron (FE) current to the work function. Since the pioneering work in 1993 [21], many

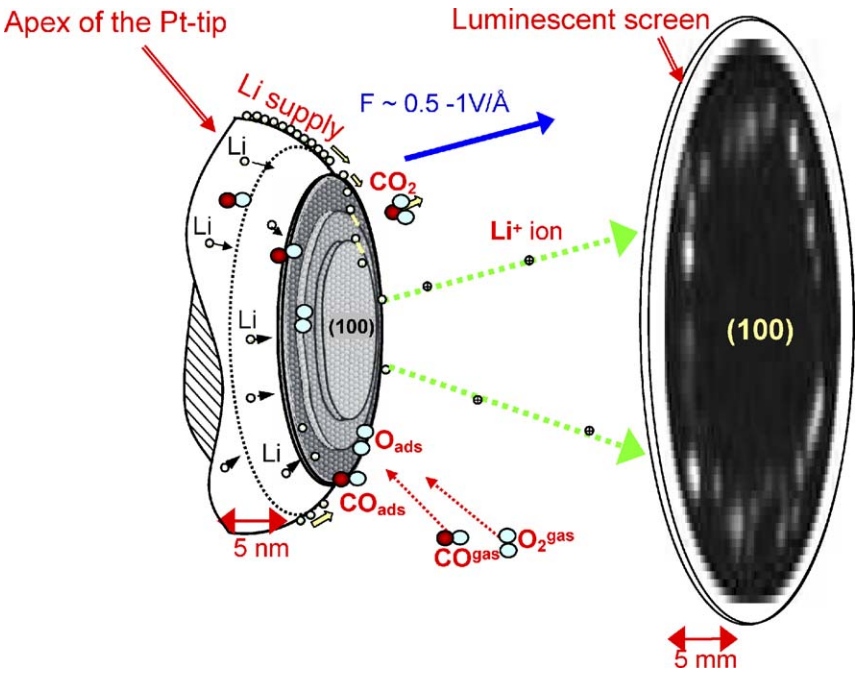

Fig. 1. Visualisation of the CO oxidation in Li-FDM. A lithium submonolayer on the shank of a field emitter tip serves as a long-lasting reservoir of Li atoms, that diffuse towards the apex of the tip and desorb from those surface sites where the local field strength is sufficient for field desorption. Li^+ ions created at the instance of field desorption are accelerated towards the screen creating a point-projection of the tip surface, similarly as in a FIM.

FEM studies of the $O/CO/Pt_{tip}$ system have been conducted. An overview can be found in [22].

3.1. "Hex" reconstruction of the Pt(100) facet

Usually, global oscillations are observed where the whole apex surface is involved. Fig. 2(a) shows a typical time dependence of the total FE current for such oscillations. The electric field necessary in FEM for the tunnelling of field electrons is about 5 V/nm and does not influence the reaction, as was convincingly shown in experiments with a pulsed field and varied duty pulses [23]. However, under certain conditions local, rather irregular oscillations can be observed on the central (100) facet with a very short cycle duration of 1–3 s only. Here we focus on a single 1.6 s long cycle. At the beginning, the Pt(100) facet is covered with O_{ad} (Fig. 2(b)). Subsequently the O_{ad} layer shrinks slowly (Fig. 2(c)) due to the reaction with CO_{ad} at the borders of the oxygen-covered surface, as also observed in a recent STM study [24]. Suddenly, the clean-off reaction removes the remaining O_{ad} and creates an area on the (100) facet with a very high local image brightness (high local FE current, Fig. 2(d)), which even exceeds that expected for a surface with the work function values of the clean Pt(100) surface in its 1×1 as well as its "hex" phase [25,26]. The only possible explanation for this effect is a local electron current increase caused by the local field enhancement due to the local transient changes in surface corrugation, which accompany the formation of the "hex" phase, as was observed by STM [27]. We will discuss below the relation between the local field enhancement (at subnanometer distances to the surface) and the peculiarities of the atomic surface corrugation.

Because of the very low sticking coefficient of $<10^{-3}$ for oxygen on the "hex" surface, this surface will immediately be covered with CO under the given conditions, which happens in fact in the next tenths of a second (Fig. 2(e)). Adsorption of CO forces the hex $\rightarrow 1\times1$ reconstruction, since CO is more strongly bound to the 1×1 surface, switching back the sticking coefficient of oxygen from $<10^{-3}$ to 0.3. Since the partial pressure of oxygen is more than two orders of magnitude larger than that of CO, this leads necessarily to the dominance of oxygen adsorption and the surface becomes covered with O_{ad} again, as can be seen in Fig. 2(f) which corresponds to the initial state shown in Fig. 2(b).

The proposed mechanism was proven in a separate titration experiment at 338 K, where a pre-adsorbed CO_{ad} layer on the tip apex surface was reacted off by oxygen which was introduced into the UHV system at 5×10^{-4} mbar. The main result of this experiment is shown in Fig. 2(g). The reaction starts in the vicinity of the (110) facet, and a sharp reaction front moves fast towards the central (100) facet. After arriving at the latter the reaction front produces a high local FE current peak comparable to that observed in the oscillation cycle, but for a somewhat longer period due to the different time scales of the fast surface clean-off reaction and of the relatively slow refilling of the surface due to the low sticking coefficient of oxygen which is characteristic for the "hex" surface that was created during the clean-off reaction. In conclusion, by using the FE imaging mode with its lateral resolution of about

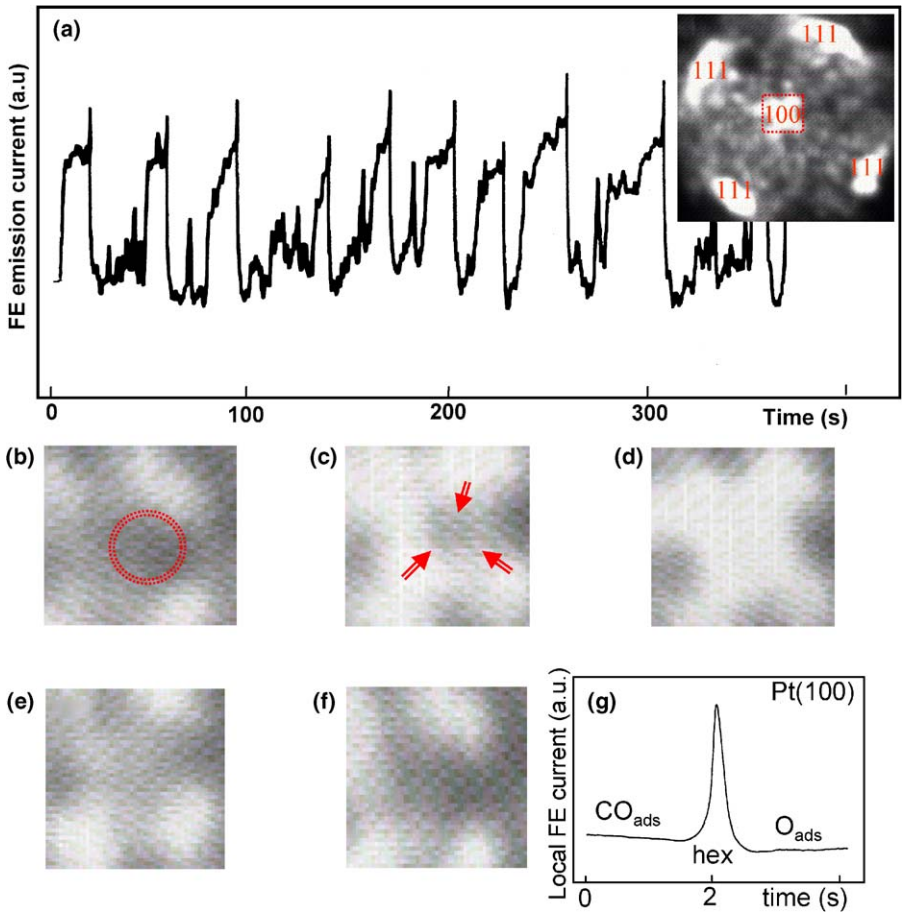

Fig. 2. Global and local oscillations in the CO oxidation reaction on the apex of an [100]-oriented Pt tip. (a) Global oscillations: total field electron current vs. time at 403 K, $p_{CO} = 1.5 \times 10^{-5}$ mbar, $p_{O_2} = 5.3 \times 10^{-4}$ mbar. The inset shows a corresponding FEM image. All crystallographic orientations are involved in the oscillations. The dotted rectangle is magnified in (b–f). (b–f) Fast local oscillations: a sequence of FE images obtained on the central (100) facet at 346 K, $p_{CO} = 2.3 \times 10^{-6}$ mbar, $p_{O_2} = 4 \times 10^{-4}$ mbar. Only the central part of the (100) region is oscillating. (b) Central Pt(100) facet covered with O_{ad} (dotted circle, ca. 10 nm ∅; dark image due to low work function). (c) Shrinkage of the O_{ad} layer due to reaction with CO. (d) Formation of the clean "hex"-reconstructed (100) surface, as indicated by the very bright image. (e) Lifted "hex"-reconstruction due to CO_{ad} layer formation. (f) Refilling of the (100) facet with O_{ads} within just one video frame (0.04 s), thus closing the cycle after 1.6 s duration [compare to (b)]. (g) Local FE current from the Pt(100) facet measured in a titration experiment. Passing the (100) area, the reaction front creates an emission peak attributed to the clean "hex" surface [compare to (d)]. The stripes in the images are due to the video-recording system.

2 nm, the attribution of the O_{ad} and CO_{ad} layer to particular states of the Pt(100) nanofacets is possible. Although the resolution of 2 nm is not really sufficient to observe directly the differences in the atomic structure of the "hex"- and 1×1 phases, the decisive step of the clean "hex" structure formation can nevertheless be reliably identified.

3.2. "Missing row" reconstruction of the Pt(110) facets

We will now concentrate on the (110) facets of the [100]-oriented tip, imaged with Li^+ ions during the oscillating CO oxidation at a similar magnitude of the applied field, but under reversed polarity. In comparison to electrons during the tunnelling process, field-desorbed lithium ions are much better spatially localized at the instance of field desorption (almost monoenergetic Li^+ ions are emitted in this mode, the FWHM of their energy distribution being less than 250 meV [28]). For this reason an extreme sensitivity of the probing Li^+ ions on the atomic structure of the surface can be expected. We note that presence of the rather rarefied Li-submonolayer (in a 0.1 ML range) on the Pt-surface does not influence the CO oxidation mechanism itself, just a slight shift of the reactive phase diagram is observed and explained using lattice-gas type model calculations [23,29]. In Fig. 3(a) the time dependence of the local image brightness collected within a ROI placed in a (110) region of a [100]-oriented tip and monitored with Li-FDM during the oscillating CO oxidation is shown ($p_{CO} = 1.8 \times 10^{-5}$ mbar, $p_{O_2} = 2 \times 10^{-4}$ mbar, $T = 490$ K). During the self-sustained oscillations in the reaction, the Li-FDM image switches periodically, with a period of ~120 s, between a circular (Fig. 3(b)) and a cross-shaped pattern (Fig. 3(c)), where the maxima of the local image brightness registered in the ROI in the (110) region correspond to the circle-like pattern, and the minima in the oscillating brightness curve to the cross-like image. In

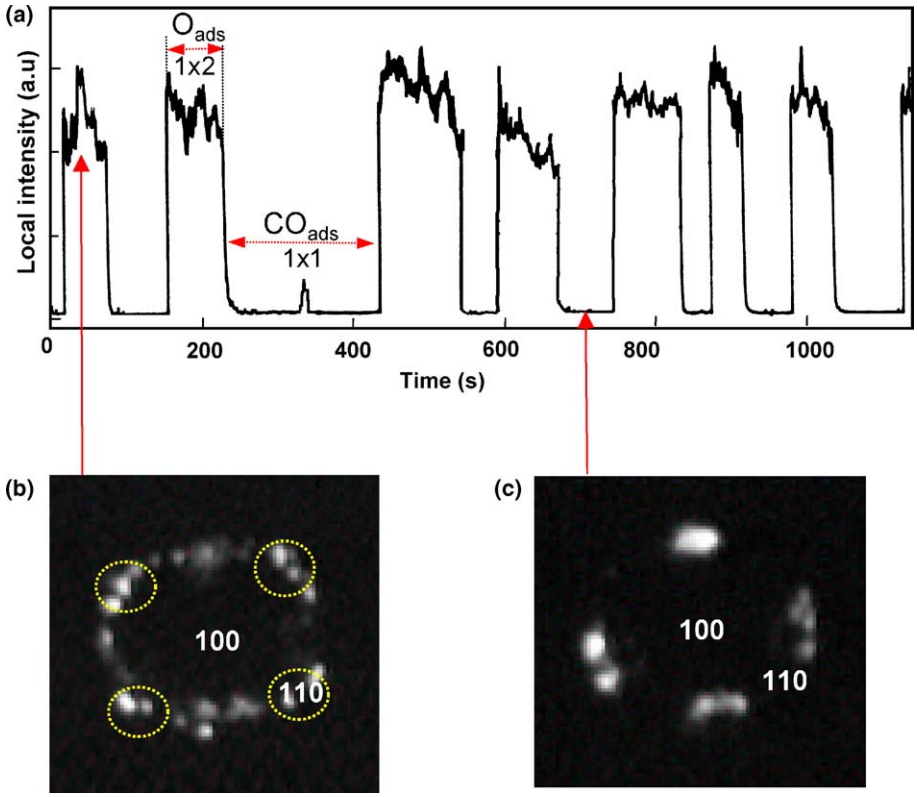

Fig. 3. The oscillating CO oxidation reaction on Pt nanofacets monitored with Li^+ ions at 490 K, $p_{CO} = 1.8 \times 10^{-5}$ mbar, $p_{O_2} = 2 \times 10^{-4}$ mbar. (a) Local intensity of the Li-FDM image in the (1 1 0) region vs. time. (b) Li-FDM image of the oxygen-covered apex of the [1 0 0]-oriented Pt tip. The dotted circles indicate the (1 1 0) regions. (c) The same for the CO-covered surface. The (1 1 0) regions remain dark (no field desorption of Li from those regions under these conditions).

order to attribute the local image brightness to adsorption of O_{ad} or CO_{ad}, titration experiments were performed under the same experimental conditions. The reaction of a pre-adsorbed O_{ad} layer with CO leads immediately to the cross-shaped pattern, and unambiguously proves that during the minima in the oscillation curve the Pt(1 1 0) facet was covered with CO. In turn, removing pre-adsorbed CO_{ad} by oxygen leads to the circle-like image with high local intensity in the (1 1 0) regions, which corresponds to the maxima in the intensity curve. This Li-FDM image brightness corresponds to much higher Li^+ desorption rate from the O_{ad}-covered surface, as compared to the CO_{ad}-covered surface where Li field desorption does not take place or is not significant (the corresponding regions of the image remain dark). Field desorption of Li from metal surfaces is well studied experimentally as well as theoretically [30,31]. These studies have demonstrated a high sensitivity of the Li^+ desorption rate on the strength of the local desorption field, which acts on the Li adatom at the instant of field desorption. Thus the explanation for the brightness enhancement observed herein in Li-FDM is a much higher local desorption field on a surface covered with O_{ad} than with CO_{ad}. In turn, the question on the origin of this enhanced desorption field arises.

In order to answer this question, we refer to our own study of the local electrostatic field distribution above individual surface atoms [32]. Using field ion appearance energy spectroscopy for the determination of the local field strengths at subnanometer distances over single atoms, the local field above surface atoms was found to depend strongly on the local surface corrugation. Fig. 4 illustrates those findings: a field ion image obtained with Ne^+ ions at 79 K from the close-packed Rh(1 0 0) surface is shown in Fig. 4(a) with the corresponding surface structure, while Fig. 4(b) shows the same for a strongly corrugated Rh(1 1 3) facet. For the less corrugated Rh(1 0 0) surface, the field strength measured 0.3–0.4 nm above the surface atoms appears to be locally enhanced by a factor of 1.27 relative to the "externally applied" field of 31 V/nm measured farther away from the surface (>1.5 nm). In turn, the local field enhancement factor measured at the "rougher" Rh(1 1 3) surface was found to be higher, namely 1.54 under at the same conditions. The different enhancement factors are attributed to the particular atomic corrugations on the respective surfaces. Details of these atomic scale measurements, of corresponding theoretical calculations, and of the physics of the field-induced redistribution of the local electron density leading to the local field enhancement are summarised in [33].

The corrugation of the non-reconstructed Pt(1 1 0) surface drawn in Fig. 4(c) is similar to the one shown in the lower corner of Fig. 4(a) for Rh(1 0 0), while the corrugation of the reconstructed Pt(1 1 0) surface (Fig. 4(d)) is similar to that exhibited in Fig. 4(b) for the Rh(1 1 3) facet.

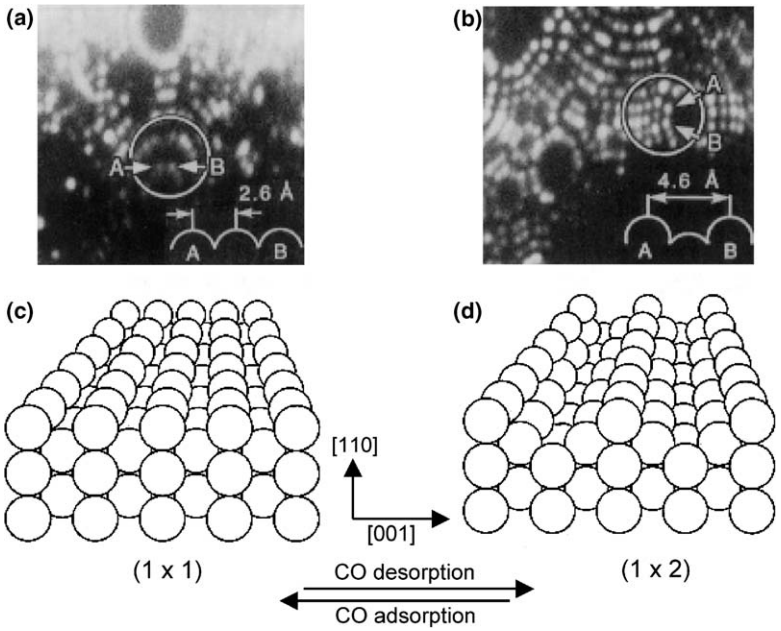

Fig. 4. Surface corrugation and local electric fields. (a) Section of a Ne field ion image at 79 K, showing a Rh(1 0 0) facet. The white circle shows the position of the probe hole. The local field enhancement factor was measured to $F_{loc}/F_0 = 1.27$. The corresponding surface corrugation A–B is also shown. (b) Same as in (a), but for a Rh(1 1 3) facet. $F_{loc}/F_0 = 1.54$. Both taken from [32]). (c) Surface corrugation of the non-reconstructed Pt(1 1 0) surface. (d) Same as in (c) but for the (1×2) "missing row" reconstruction. Due to the stronger corrugation a higher local field enhancement factor is expected than for the (1×1) structure.

This strongly suggests that for the same value of the externally applied tip voltage different local field enhancements, caused by differently strong corrugations, will provide different local desorption fields for the Li atoms on these two differently corrugated surfaces. By adjustment of the externally applied field to a value just sufficient for the field desorption of Li from the oxygen-covered 1×2 surface, no Li^+ emission from the CO-covered and much smoother 1×1 surface was observed since the local field strength does not suffice for Li field desorption. This is another evidence for two different structures on the same Pt(1 1 0) nm-sized facet caused by different CO coverages. The switching between the 1×1 and 1×2 structures modifies the sticking coefficient for oxygen, thus providing the negative feedback as described above for the macroscopic single crystal surfaces.

4. Conclusions

Using the apex of a Pt field emitter tip as a well-defined model for a catalytically active Pt nanoparticle, the materials gap has been partially bridged in the sense that the feedback mechanism of the oscillating CO oxidation reaction in a heterogeneous nm-sized system was compared with that known from macroscopic single crystals. The experiments provide the evidence that also in case of the nm-sized facets on the curved surface of a Pt tip with its different crystallographic orientations, where the reaction can be coupled via surface diffusion, the feedback occurs via the lifted reconstruction of the Pt(1 0 0) and (1 1 0) facets, similar to macroscopic single crystal surfaces.

Acknowledgements

The authors gratefully acknowledge financial support by the Land Sachsen-Anhalt. V.V.G. and W.D. acknowledge partial support by the RFBR (grant no. 05-03-32971) and by the INTAS (project no. 04-78-7183), correspondingly.

References

[1] L.H. Germer, A.U. MacRae, Proc. Nat. Acad. Sci. USA 48 (1962) 997.
[2] R. Imbihl, S. Ladas, G. Ertl, Surf. Sci. 206 (1988) L903.
[3] G. Ertl, P.R. Norton, J. Rüstig, Phys. Rev. Lett. 49 (1982) 177.
[4] G. Ertl, Surf. Sci. 299/300 (1994) 742.
[5] M. Eiswirth, G. Ertl, Pattern formation on catalytic surfaces, in: R. Kapral, K. Showalter (Eds.), Chemical Waves and Patterns, Kluwer, Dordrecht, 1995.
[6] K. Krischer, M. Eiswirth, G. Ertl, J. Chem. Phys. 96 (1992) 9161.
[7] M. Bär, C. Zülicke, M. Eiswirth, G. Ertl, J. Chem. Phys. 96 (1992) 8595.
[8] U.F. Frank, in: L. Rensing, N.I. Jaeger (Eds.), Temporal Order, Springer, Berlin, 1985.
[9] A.T. Pasteur, X.C. Guo, T. Ali, M. Gruyters, D.A. King, Surf. Sci. 366 (1996) 564.
[10] P.R. Norton, K. Griffits, P.E. Bindner, Surf. Sci. 138 (1984) 125.
[11] N. Freyer, M. Kiskinova, G. Pirug, H.P. Bonzel, Surf. Sci. 166 (1986) 206.
[12] R. Imbihl, G. Ertl, Chem. Rev. 95 (1995) 697, and references therein.
[13] M. Eiswirth, G. Ertl, Surf. Sci. 177 (1986) 90.
[14] Y. Suchorski, J. Beben, E.W. James, J.W. Evans, R. Imbihl, Phys. Rev. Lett. 82 (1999) 1907.
[15] V. Gorodetskii, J. Lauterbach, H.H. Rotermund, J.H. Block, G. Ertl, Nature. 370 (1994) 276.
[16] Q.J. Gao, T.T. Tsong, Phys. Rev. B 36 (1987) 2547.
[17] C. Voss, A. Gausmann, N. Kruse, Appl. Surf. Sci. 67 (1993) 142.

[18] V. Gorodetskii, W. Drachsel, J.H. Block, Appl. Surf. Sci. 76/77 (1994) 122.
[19] V.K. Medvedev, Y. Suchorski, J.H. Block, Appl. Surf. Sci. 87/88 (1995) 159.
[20] Y. Suchorski, J. Beben, Progr. Surf. Sci. 74 (2003) 3.
[21] V.V. Gorodetskii, J.H. Block, W. Drachsel, M. Ehsasi, Appl. Surf. Sci. 67 (1993) 198.
[22] V.V. Gorodetskii, V.I. Elokhin, J.W. Bakker, B.E. Nieuwenhuys, Catal. Today 105 (2005) 183.
[23] Y. Suchorski, R. Imbihl, V.K. Medvedev, Surf. Sci. 401 (1998) 392.
[24] J. Wintterlin, S. Völkening, T.V.W. Janssens, T. Zambelli, G. Ertl, Science 278 (1997) 1931.
[25] J. Radnik, F. Gitmans, B. Pennemann, K. Oster, K. Wandelt, Surf. Sci. 287/288 (1993) 330.
[26] R.J. Behm, P.A. Thiel, P.R. Norton, G. Ertl, J. Chem. Phys. 78 (1983) 7437.
[27] T. Gritsch, D. Coulman, R.J. Behm, G. Ertl, Phys. Rev. Lett. 63 (1989) 1086.
[28] V.K. Medvedev, Y. Suchorski, J.H. Block, J. Vac. Sci. Technol. B 13 (1995) 621.
[29] N. Pavlenko, P.P. Kostrobij, Y. Suchorski, R. Imbihl, Surf. Sci. 489 (2001) 29.
[30] Y. Suchorski, V.K. Medvedev, J.H. Block, Phys. Rev. B 51 (1995) 4734.
[31] Y. Suchorski, V.K. Medvedev, J.H. Block, R.L.C. Wang, H.J. Kreuzer, Phys. Rev. B 53 (1996) 4109.
[32] W.A. Schmidt, N. Ernst, Y. Suchorski, Appl. Surf. Sci. 67 (1993) 101.
[33] Y. Suchorski, W.A. Schmidt, N. Ernst, J.H. Block, H.J. Kreuzer, Progr. Surf. Sci. 48 (1995) 121.